PRAMANA
— journal of
physics

© Printed in India

Vol. 48, No. 4,
April 1997
pp. 871–882

Characterization of chaos in a serrated plastic flow model

S V M SATYANARAYANA, V SRIDHAR and S KOKA
Materials Science Division, Indira Gandhi Centre for Atomic Research, Kalpakkam 603 102, India

MS received 23 May 1996; revised 30 December 1996

Abstract. We report new results on a dynamical model of serrated yielding. These essentially pertain to the full spectrum of Lyapunov exponents of the non-linear (chaotic) model and fractal characterization of the associated strange attractor. The power spectrum of scalar time series extracted from the phase space trajectories decays exponentially with increase of frequency and the decay constant is found proportional to the Kolmogorov–Sinai entropy.

Keywords. Chaos; Lyapunov exponents; fractal measures; time series; Kolmogorov–Sinai entropy; plastic flow.

PACS Nos 05·45; 62·20; 83·50

1. Introduction

The phenomenon of repeated and discontinuous yielding of materials under stress is of considerable interest, mainly because it is related to the basic issue of stability of materials. This phenomenon manifests itself as serrations in the stress-strain curve when a specimen of the material is subjected to constant strain rate. There exists a rich literature on the subject of serrated yielding, also known by various names like, jerky flow, Portevin–Le Chatelier (PLC) effect etc., addressing both theoretical [1–5] and experimental aspects [6–9]. Several models have been proposed to understand serrated yielding that include the solute-atom hypothesis of Cottrell [1], an improvement proposed by McCormic [2] and Van den Beukel [3, 4], the Coulomb friction model of Bodner and Rosen [5], to name only a few. In this paper we shall be concerned with a nonlinear dynamical model proposed by Ananthakrishna [10] in the early eighties. This model, which we shall refer to as Anantha oscillator, seeks to explain the phenomenon of serrated yielding as occurring due to nonlinear interactions amongst three types of dislocations namely the mobile, the immobile and the ones surrounded by a cloud of solute atoms. Anantha oscillator has explained several experimental observations [10–12], principal amongst which is jumps in the creep curves. An important prediction of the model is that the dynamics underlying the plastic flow is chaotic for certain strain rates. Recently Anantha oscillator has attracted renewed attention owing mainly to the fact that two independent studies of two different experimental data on serrated yield [13–15] have shown that there is *prima facie* evidence for a low dimensional chaotic dynamical mechanism responsible for and underlying the experimental scalar time series. This has motivated us to revive interest in this model and carry out some of the unfinished tasks like, estimating the full spectrum of Lyapunov exponents and characterizing the invariant measure of the strange attractor in terms of scaling exponents of the partition function, generalized Renyi entropy dimensions and the spectrum of singularities. We also verify the validity of the Kaplan–Yorke conjecture [16] that relates the (dynamical) Lyapunov exponents to the (static) fractal measure of the strange attractor. Also a scalar time series extracted from this continuous time chaotic dynamical system, has a power spectrum that decays exponentially at large frequencies. A recent study [17] of different chaotic systems showed that the exponential decay constant is nearly proportional to the Kolmogorov–Sinai (KS) entropy, given by the sum of the positive Lyapunov exponents. We demonstrate that such a relation between the exponential decay constant, which is a characteristic of the stationary time series and the Lyapunov exponents, which characterize the unstable dynamics, holds good for Anantha oscillator also.

This paper is organized as follows. In §2, we present a set of four coupled nonlinear equations that form the central descriptor of the Anantha oscillator, and describe briefly the variables of the equations of motion and the control parameters. We state the nature of the chaotic mechanism predicted by the model and the values of the control parameter that lead to chaotic solutions. Section 3 contains a brief description of the computational procedure adopted for estimating the Lyapunov exponents. In §4, we characterize the fractal measures of the strange attractor. In §5, we report results on Lyapunov dimension and verify the Kaplan–Yorke conjecture. We construct several scalar time series from the four dimensional phase space trajectory, and for each, calculate the constant characterizing the exponential decay of the power spectrum at large frequencies. We show that the exponential decay constant is same for all the time series and is proportional to the Kolmogorov–Sinai entropy. These are described in §6. A summary of the principal conclusions of the study is given in §7.

2. Model for serrated yielding: Anantha oscillator

The Anantha model considers three types of dislocations; the mobile, the immobile and the ones with cloud of solute atoms. The corresponding scaled densities are denoted by x_1, x_2 and x_3 respectively. Using well-known dislocation reaction mechanisms, the rate equations for the densities of dislocations were set up and then coupled to machine equation for the rate of change of applied stress, x_4 [10]. The set of four coupled nonlinear equations that describe the dynamics are

$$\frac{\mathrm{d}x_1}{\mathrm{d}t} = x_4^m x_1 - bx_1^2 - ax_1 + x_2 - x_1x_2, \tag{1}$$

$$\frac{\mathrm{d}x_2}{\mathrm{d}t} = b(bx_1^2 - x_2 - x_1x_2 + ax_3), \tag{2}$$

$$\frac{\mathrm{d}x_3}{\mathrm{d}t} = c(x_1 - x_3), \tag{3}$$

$$\frac{\mathrm{d}x_4}{\mathrm{d}t} = d(e - x_4^m x_1), \tag{4}$$

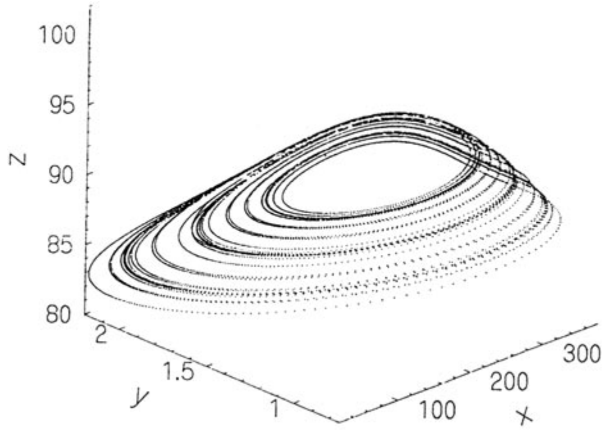

Figure 1. Strange attractor of Anantha oscillator.

where a refers to the concentration of the solute atoms; b, the strength of reactivation of immobile dislocations; c^{-1}, the time scales over which the slowing down occurs; d, the effective modulus; e, the applied strain rate and m, the velocity exponent which describes the dependence of velocity of dislocations on the stress. For a certain range of values of the parameters, the steady state is unstable. Analysis is carried out for these parameter values and the applied strain rate e is taken as the drive parameter.

There have been several studies on Anantha model [10–12, 18–20]. The system exhibits periodic solutions called limit cycles [18]. In a certain range of the applied strain rate e, the model exhibits chaotic oscillations through period doubling route. Feigenbaum number corresponding to the period doubling bifurcation is 4·669. The strange attractor associated with the chaotic dynamics was also constructed and figure 1 depicts a three dimensional section of the strange attractor. In this paper we compute the full Lyapunov spectrum and the fractal measures of the associated strange attractor, for the following values of the parameters: $a = 0{\cdot}7$, $b = 0{\cdot}002$, $c = 0{\cdot}008$, $d = 0{\cdot}0001$, $m = 2{\cdot}0$ and $e = 184{\cdot}9$. For this purpose the four nonlinear equations were solved numerically employing fourth order Runge-Kutta technique with time step of 0.1. First 40,000 time steps of evolution were treated as transients and rejected.

3. Lyapunov exponents

Lyapunov exponents quantify the exponential divergence/convergence of the neighbouring trajectories. We estimate the Lyapunov exponents employing the method described by Wolf [21].

Consider the four dimensional continuous time dynamical system described by equations (1–4). These can be expressed as

$$\frac{d\mathbf{x}}{dt} = \mathbf{f}(\mathbf{x}). \tag{5}$$

Let $\mathbf{x}(t)$ denote a trajectory in the four dimensional phase space, residing on the strange attractor, evolving from an initial point $\mathbf{x}(0) = \mathbf{x}_0$. Also consider a four dimensional infinitesimal sphere of initial conditions of radius unity surrounding $\mathbf{x}_0$. After time t, this sphere would get distorted by the equations of motion, to a four dimensional ellipsoid with principal axes, $l_1 \geqslant l_2 \geqslant l_3 \geqslant l_4$. The size of $\{l_i;\ i = 1,4\}$ represents the convergence ($l_i < 1$) or the divergence ($l_i > 1$) of the trajectories emanating from the neighbourhood of $\mathbf{x}_0$. Formally we write $l_i = \exp\ (\lambda_i t)$, where $\{\lambda_i;\ i = 1,4\}$ are the Lyapunov exponents. Thus we have,

$$\lambda_i = \lim_{t\to\infty} \frac{1}{t} \ln(l_i) \tag{6}$$

and $\lambda_1 \geqslant \lambda_2 \geqslant \lambda_3 \geqslant \lambda_4$

We start with four orthonormal vectors $\{\xi^\beta(0);\ \beta = 1,4\}$, located at $\mathbf{x}(0)$. These vectors, which define a sphere of initial conditions, is evolved up to T via the linearized version of the equation of motion

$$\frac{\mathrm{d}\xi_i^\beta(t)}{\mathrm{d}t} = \sum_j F_{ij}\xi_j^\beta(t), \tag{7}$$

where $F_{ij} = \partial f_i/\partial x_j$. $|\xi_i^\beta(T) - \xi_i^\beta(0)|$ gives $(l_i)_1$ in time T, for $i = 1,4$. At T we re-orthonormalize $\xi^\beta(T)$ using Gram–Schmidt orthogonalization procedure. Using this as a unit sphere of initial conditions at T, the linearized evolution is continued up to $2T$ and $(l_i)_2$ is computed. This procedure is continued N times and the average Lyapunov exponents are then computed as

$$\lambda_i = \frac{1}{N}\sum_{j=1}^{N} \frac{\ln(l_i)_j}{T}. \tag{8}$$

These are given in table 1. The error bars on the Lyapunov exponents have been obtained by monitoring the sample fluctuations.

We observe that the exponent λ_1 is positive, indicative of chaos. λ_2 is positive, but very small. We conclude that λ_2 characterizes the tangential flow [23]. The other two exponents λ_3 and λ_4 are negative. Also the sum of the Lyapunov exponents is negative indicating that the system is dissipative (the phase space volume is contracting on the average).

4. Fractal measures of the strange attractor

To calculate the fractal measures of the strange attractor we evolve a dynamical trajectory for N time steps; N is taken adequately large to span the strange attractor

Table 1. Numerical results.

Model	Parameters	λ_i	d_{KY}	$\Sigma_i \lambda_i^+$	μ	$\mu/\Sigma_i \lambda_i^+$
Anantha	$a = 0{\cdot}7$					
oscillator	$b = 0{\cdot}002$	$\lambda_1 = 0{\cdot}00887 \pm 0{\cdot}0003$				
	$c = 0{\cdot}008$	$\lambda_2 = 0{\cdot}00088 \pm 0{\cdot}0002$				
	$d = 0{\cdot}0001$	$\lambda_3 = -0{\cdot}03688 \pm 0{\cdot}0002$	$2{\cdot}27 \pm 0{\cdot}15$	$0{\cdot}00975$	$0{\cdot}0097$	$0{\cdot}9949$
	$e = 184{\cdot}9$	$\lambda_4 = -0{\cdot}60051 \pm 0{\cdot}0001$				
	$m = 2{\cdot}0$					

reasonably well. We determine the smallest four dimensional paralellopiped that can hold all the N discrete phase space points of the dynamical trajectory. The coordinates of these points are scaled in such a way that they are contained in a hyper-cube of unit side. This unit hyper-cube is further divided into non-overlapping hyper-cubes each of side, ε, where $\varepsilon = N^{-1/4}$. Let $p_i(\varepsilon) = n_i/N$ denote the fractional number of phase space points that are contained within the ith hyper-cube. The partition function is defined as

$$Z(q,\varepsilon) = \sum_i p_i^q(\varepsilon), \tag{9}$$

where the sum over i runs only over the non-empty boxes, and $-\infty < q < +\infty$. For calculating partition function, we have employed the fast box counting algorithm, see [24]. The scaling ansatz reads as

$$Z(q,\varepsilon) \overset{\varepsilon \to 0}{\sim} \varepsilon^{\tau(q)}. \tag{10}$$

Figure 2(a) depicts ln $Z(q,\varepsilon)$ versus $\ln(\varepsilon)$ for representative values of q. For a given q, all the points fall on a straight line, verifying the scaling ansatz. The slope of the straight line yields the scaling exponent $\tau(q)$. Due to limitations on the computer resources, we could verify the scaling ansatz over a small range of ε only. Employing an alternate technique [25] we could establish the scaling behaviour over a range of resolution exceeding one order of magnitude, see figure 2(b). However, there are numerical problems associated with this technique which are discussed in the appendix. Figure 3 depicts the variation of $\tau(q)$ with q. Scaling exponent, $\tau(q)$ is not linear and exhibits well defined change of slope, showing that the invariant dynamical measure on the strange attractor is a multifractal. The generalized Renyi dimensions $D(q)$ are given by

$$D(q) = \frac{\tau(q)}{q-1} \tag{11}$$

for $q \neq 1$. For $q = 1$ we calculate $D(q)$ by taking the limit $q \to 1$. The variation of $D(q)$ with q is as depicted in figure 4. We find $D(q)$ is a monotonically non-increasing function of q. For $q = 0, 1$ and $2, D(q)$ are known as capacity, information and correlation dimensions, respectively, and these are 2·100, 1·882 and 1·799.

The singularity spectrum is obtained by taking the Legendre transform of $\tau(q)$, as below

$$f(\alpha) = -\tau(q) + q\alpha, \tag{12}$$

$$\alpha = \frac{\mathrm{d}\tau(q)}{\mathrm{d}q}. \tag{13}$$

Figure 5 shows the singularity spectrum of $f(\alpha)$ versus α. It is convex, with a single maximum at $q = 0$ with $f(\alpha(q = 0)) = D(0)$. We find that $\alpha_{max} = D(q \to -\infty) = 3{\cdot}98$, indicating that the rarest region is very nearly (phase) space filling with fractal dimension 3·98. On the other hand we find that $\alpha_{min} = D(q \to \infty) = 1{\cdot}77$, indicating that the densest region is a fractal set of dimension 1·77.

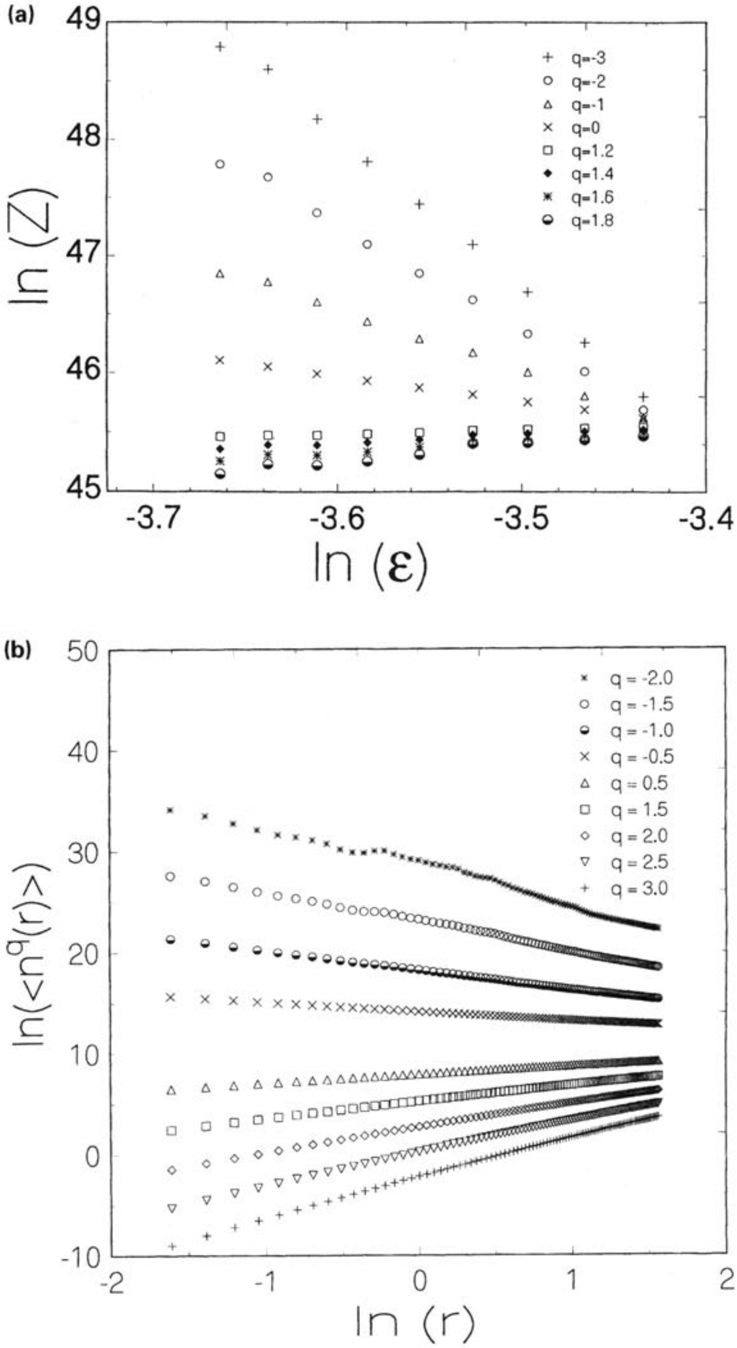

Figure 2. (a) Scaling behaviour of the partition function. **(b)** Scaling behaviour of the moments (see appendix).

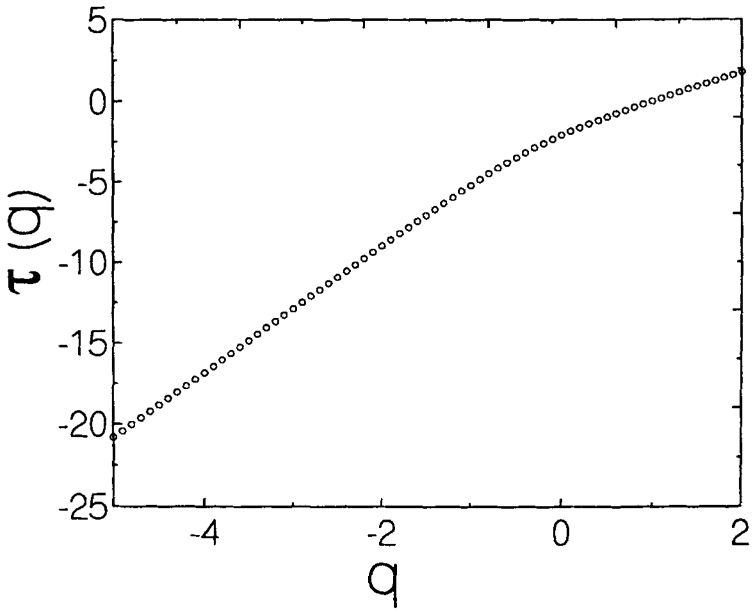

Figure 3. The scaling exponent.

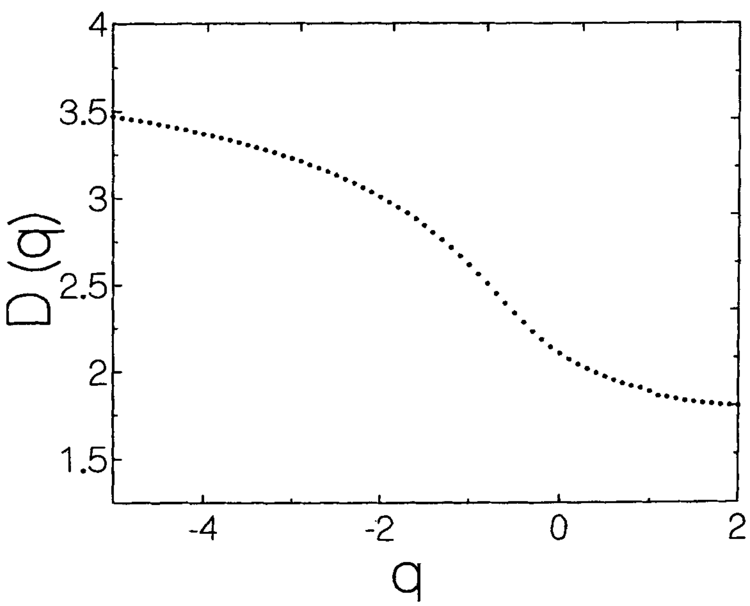

Figure 4. Generalized Renyi dimensions.

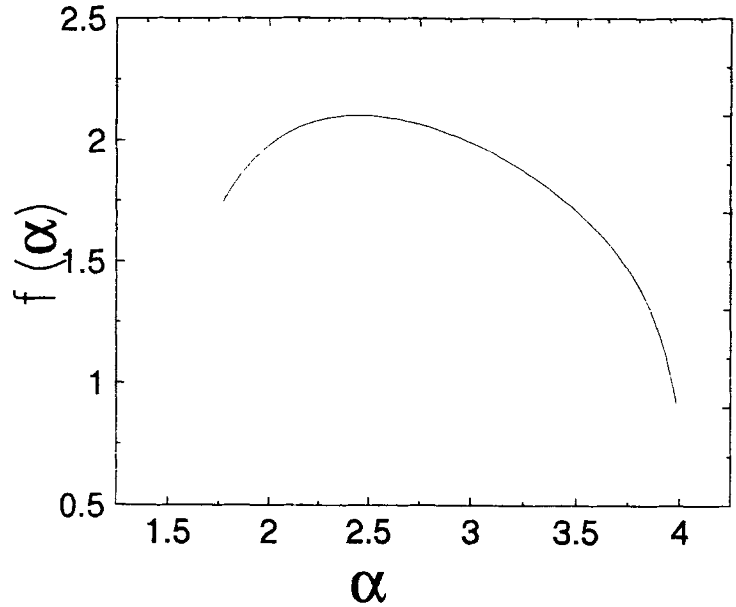

Figure 5. Singularity spectrum.

5. Lyapunov dimension

The Lyapunov spectrum is closely related to the fractal dimension of the associated strange attractor. It has been conjectured by Kaplan and Yorke [16] that Lyapunov dimension d_{KY} is related to the Lyapunov spectrum as given by

$$d_{KY} = j + \sum_{i=1}^{j} \frac{\lambda_i}{|\lambda_{j+1}|}, \tag{14}$$

where j is determined by the condition

$$\sum_{i=1}^{j} \lambda_i > 0 \quad \text{and} \quad \sum_{i=1}^{j+1} \lambda_i < 0. \tag{15}$$

The Lyapunov dimension calculated for this model is in the range 2·122 to 2·423. The spread in the calculated value of d_{KY} is due to the error bars on λ_i (see table 1). Within numerical accuracy, the Lyapunov dimension matches with the capacity dimension $D(0)$, verifying the conjecture of Kaplan and Yorke.

6. Decay of the power spectrum

It is generally believed that the power spectrum of a time series taken from a continuous time dynamical system decays exponentially at high frequencies [22]. We can represent the decay as

$$P(f) \sim e^{-f/\mu}, \tag{16}$$

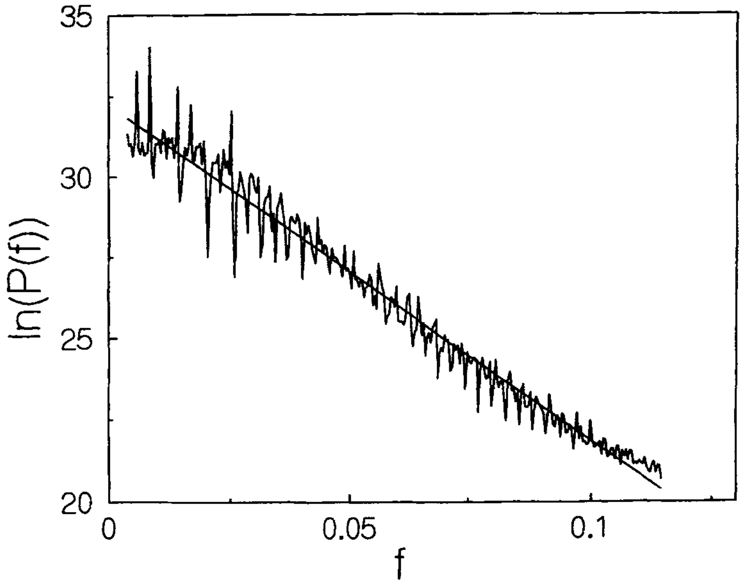

Figure 6. Exponential decay of the averaged power spectrum corresponding to time series $x_1(t)$.

where μ is the decay constant. It has been shown recently [17] that μ is proportional to the Kolmogorov–Sinai entropy given by the sum of the positive Lyapunov exponents. The ratio of μ to Kolmogorov–Sinai entropy is found to fall within a narrow range of 0·64 to 2·46 for a variety of systems exhibiting chaos with attractor dimensions varying from 2 to 20.

We have studied the exponential decay of the time series taken from Anantha model, whose attractor dimension is 2·1. Superimposed on the exponential decay are oscillations. These oscillations get largely smoothened out when we average the power spectrum over several time series. Figure 6 depicts the power spectrum for $x_1(t)$, averaged over several time series. The exponential decay is clearly seen in the picture. The decay constant μ has been calculated and the ratio of μ to K-S entropy is found to be 0·9949.

Discretely sampled data results in aliasing of the power spectrum as given by

$$P_a(f) = \sum_{j=-\infty}^{+\infty} P_N(f \pm 2jf_c), \tag{17}$$

where f is the frequency and $f_c = (2\delta t)^{-1}$ is Nyquist frequency. δt is the sampling interval. $P_N(f)$ is the power spectrum of the time series of size N and $P_a(f)$ is the aliased power spectrum. Invariably, we find that the exponential decay is followed by a power law flattening. This feature seems to be generic in character in the sense that finite size discrete time series extracted from a variety of chaotic oscillators exhibit this property. Such power law flattening can also be seen clearly in the figures of the power spectrum

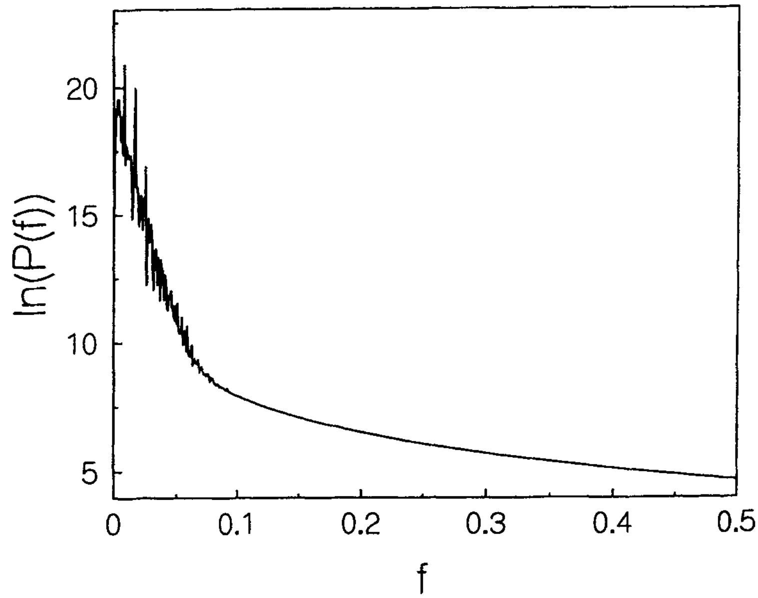

Figure 7. Full power spectrum of $x_4(t)$ exhibiting an exponential decay followed by a power law flattening.

depicted in [17]. For the Anantha oscillator, figure 7 shows a power spectrum that decays exponentially followed by a power law flattening. An interesting question in this context relates to the origin of the power law flattening. A recent study [26] has shown that the decay is $1/f^2$ after correcting analytically for aliasing arising due to finite sampling interval. Also this study suggests that this portion of the tail goes to zero in the limit of the length of the time series going to infinity, demonstrating that the observed power law flattening is an artifact of the finite size, and the true power spectrum is indeed band width limited with exponential decay at the far end.

7. Summary and conclusions

We have (i) studied the Anantha oscillator which has been proposed to model the chaotic behaviour of serrated yielding phenomenon, (ii) calculated the full spectrum of Lyapunov exponents for this model and (iii) characterized the fractal measures of strange attractor. We find that power spectrum of the time series extracted from the Anantha oscillator decays exponentially at large frequencies and the calculated exponential decay constant is proportional to Kolmogorov–Sinai entropy.

Acknowledgements

The authors are grateful to K P N Murthy and M C Valsakumar for suggesting this problem and for many useful discussions. One of the authors (SK) acknowledges CSIR, New Delhi for a postdoctoral fellowship.

Appendix

The fractal measures of the Anantha attractor were calculated in §4, employing the traditional box counting algorithm incorporating recent improvements suggested in [24]. These improvements helped us overcome largely, the problem of (computer) memory requirements and rendered possible fractal characterization of the Anantha attractor. Despite these improvements we could establish the scaling ansatz over a small range of r only, due to the fact that we set $r = N^{-1/4}$ for numerical stability, where N is the length of the dynamical trajectory. There are alternate numerical techniques introduced for fractal characterization of chaotic strange attractor and we consider below one of them proposed by Paladin and Vulpiani [25].

We define the number of points in a four dimensional ball of radius r centered at $\mathbf{x}_i$ as

$$n_i(r) = \operatorname*{Lt}_{N\to\infty} \frac{1}{N-1} \sum_{j=1(j\neq i)}^{N} \Theta(r - |\mathbf{x}_i - \mathbf{x}_j|), \tag{A1}$$

where Θ is the usual Heaviside step function. We then introduce a set of exponents, $\phi(q)$ under the scaling ansatz

$$\langle n^q(r)\rangle = \operatorname*{Lt}_{M\to\infty} \frac{1}{M} \sum_{i=1}^{M} n_i^q(r) \underset{r\to 0}{\sim} r^{\phi(q)}. \tag{A2}$$

In figure 2(b), we establish numerically the scaling ansatz for values of r varying more than an order of magnitude. We evolve the trajectory for $N = 2^{20}$ time steps and take the resolution r_0 to be the minimum of the distances between any two phase space points. We let r vary from $\approx 10r_0$ to $\approx 1000r_0$. We find that averaging over $M(\ll N)$ randomly chosen centers is adequate to determine $\phi(q)$. Anantha oscillator has a hole in the interior; hence most of the centers selected randomly, fall on the inner or outer surface of the attractor and as a result most of the four dimensional balls are sparse: fractal dimensions are hence underpredicted. In fact we found that if we take the number of centers as low as 1000, the fractal dimension, $D(0)$ is 1·3. However $D(0)$ increases with increasing M and saturates at 1·9 for $M \geqslant 25000$, which is still 10% less than the box counting dimension. We would remark that this technique has a tendency to underpredict the fractal dimension especially when the strange attractor encloses a hole, as in the case of Anantha oscillator. Nevertheless, we find that $\phi(q)$ is nonlinear in q, $D(q)$ is monotonic and $f(\alpha)$ upward convex.

We are presenting the results on $\tau(q)$, $D(q)$ and $f(\alpha)$ obtained from the improved box counting algorithm. The estimates of fractal characteristics from box counting algorithm are known to be robust if we link the linear dimension of the box to the length of the dynamical trajectory (see [27]). This appendix is intended to serve a limited purpose of establishing the scaling ansatz over a longer range (see figure 2(b)).

References

[1] A H Cottrell, *Philos. Mag.* **44**, 829 (1953)
[2] P G McCormic, *Acta Metall.* **219**, 351 (1972)
[3] A Van den Beukel, *Phys. Status Solidi* **A30**, 197 (1975)
[4] A Van den Beukel, *Acta Metall.* **28**, 965 (1975)

[5] S R Bodner and A Rosen, *J. Mech. Phys. Solids* **15**, 63 (1967)
[6] E Pink and A Grinberg, *Mater. Sci. Engg.* **51**, 1 (1981)
[7] G G Saha, P G McCormic and P Rama Rao, *Mater. Sci. Engg.* **62**, 187 (1984)
[8] S Venkadesan, C Phaniraj, P V Sivaprasad and P Rodriguez, *Acta Metall. Mater.* **40**, 569 (1992)
[9] S Venkadesan, S Venugopal, P V Sivaprasad and P Rodriguez, *Mater. Trans. Jpn. Inst. Met.* **33**, 1040 (1992)
[10] G Ananthakrishna and M C Valsakumar, *J. Phys.* **D15**, L171 (1982)
[11] G Ananthakrishna and D Sahoo, *J. Phys.* **D14**, 2081 (1981)
[12] G Ananthakrishna and D Sahoo, *J. Phys.* **D14**, 2091 (1981)
[13] G Ananthakrishna, *Scr. Metall. Mater.* **29**, 1183 (1993)
G Ananthakrishna, C Fressengeas, M Grosbars, J Vergnol, C Engelke, J Plessing, H Neuhäuser, E Bouchaud, J Planés and L P Kubin, *Scr. Metall. Mater.* **32**, 1731 (1995)
[14] S Venkadesan, K P N Murthy and M C Valsakumar, in Non Linear Phenomena in Materials Science III – Instabilities and Patterning, *Solid State Phenomena* edited by G Ananthakrishna, L P Kubin and G Martin (SCITEC Publications, 1995) vol. 42–43, p. 287
S Venkadesan, M C Valsakumar, K P N Murthy and S Rajasekar, *Phys. Rev.* **E54**, 611 (1996)
[15] G Ananthakrishna and S J Noronha, in Nonlinear phenomena in Materials Science III – Instabilities and Patterning, *Solid State Phenomena* edited by G Ananthakrishna, L P Kubin and G Martin (SCITEC Publlications, 1995) vols 42–43, p. 277
[16] David A Russel, James D Hanson and Edward Ott, *Phys. Rev. Lett.* **45**, 1175 (1980)
[17] David E Sigeti, *Physica*, **D82**, 136 (1995)
[18] M C Valsakumar and G Ananthakrishna, *J. Phys.* **D16**, 1055 (1983)
[19] G Ananthakrishna and M C Valsakumar, *Phys. Lett.* **A95**, 69 (1983)
[20] G Ananthakrishna and T M John, *Directions in chaos* edited by Hao Bai-lin (World Scientific, 1990) p. 133
[21] Alan Wolf, Jack B Swift, Harry L Swinney and John A Vastano, *Physica*, **D16**, 285 (1986)
[22] D Sigeti and W Horsthemke, *Phys. Rev.* **A35**, 2276 (1987)
[23] G Ananthakrishna (1995) (personal communication)
[24] Larry S Liebovitch and Tibor Toth, *Phys. Lett.* **A141**, 386 (1989)
[25] G Paladin and A Vulpiani, *Phys. Rep.* **156**, 147 (1987)
[26] M C Valsakumar, S V M Satyanarayana and V Sridhar (1996) (unpublished)
[27] K P N Murthy, L K Galos, P Argyrakis and K W Kehr, *Phys. Rev.* **E54**, 1 (1996)
K P N Murthy, S Rajasekar and K W Kehr, *J. Phys.* **A27**, L107 (1994)